Published in final edited form as:
J Phys Chem C Nanomater Interfaces. 2010 November 18; 114(45): . doi:10.1021/jp105807r.

Influence of Gold Nanoshell on Hyperthermia of Super Paramagnetic Iron Oxide Nanoparticles (SPIONs)

Faruq Mohammad[1,2], **Gopalan Balaji**[1], **Andrew Weber**[1], **Rao M. Uppu**[2], and **Challa S. S. R. Kumar**[1,*]

[1]Center for Advanced Microstructures & Devices, Louisiana State University, 6980 Jefferson Highway, Baton Rouge, LA 70806. USA

[2]Environmental Toxicology, Southern University and A&M College, Baton Rouge, LA 70813, USA.

Abstract

Gold nanoshell around super paramagnetic iron oxide nanoparticles (SPIONs) was synthesized and small angle X-ray scattering (SAXS) analysis suggests a gold coating of approximately 0.4 to 0.5 nm thickness. On application of low frequency oscillating magnetic fields (44 – 430 Hz), a four- to five-fold increase in the amount of heat released with gold-coated SPIONs (6.3 nm size) in comparison with SPIONs (5.4 nm size) was observed. Details of the influence of frequencies of oscillating magnetic field, concentration and solvent on heat generation are presented. We also show that, in the absence of oscillating magnetic field, both SPIONs and SPIONs@Au are not particularly cytotoxic to mammalian cells (MCF-7 breast carcinoma cells and H9c2 cardiomyoblasts) in culture, as indicated by the reduction of 3-(4,5-dimethylthiazol-2-yl)-5-(3-carboxymethoxyphenyl)-2-(4-sulfophenyl)-2*H*-tetrazolium by viable cells in a phenazine methosulfate-assisted reaction.

Keywords

Gold Nanoshell; SPIONs@Au Nanoparticles; Magnetic Nanoparticles; Hyperthermia

INTRODUCTION

Superparamagnetic iron oxide nanoparticles (SPIONs) are one of the most important classes of magnetic nanomaterials that are finding increasing applications in biomedicine ranging from cell labeling, [1] bio-separation, [2] bio-sensing, [3] medical diagnosis [4] and therapy.

*CORRESPONDING AUTHOR FOOTNOTE Prof. Challa S. S. R. Kumar, Center for Advanced Microstructures & Devices, Louisiana State University, 6980, Jefferson Highway, Baton Rouge, LA 70806; Tel:225-578-9320; Fax: 225-578-6954.

SUPPORTING INFORMATION AVAILABLE

(1) (a) HRTEM images and size distribution for SPIONs and SPIONs@Au. From the HRTEM data, the mean size distributions of these particles were found to be in the order of 5.4 ± 0.4, 6.3 ± 0.7 respectively. (b) EDAX image for SPIONs@Au and the quantitative information of gold on the surface of Fe_3O_4 nanoparticles obtained from EDAX. (2) UV-Visible spectrum for (a) SPIONs and (b) SPIONs@Au in toluene solution. (3) SAXS analysis showing the scattering intensity and size distribution of SPIONs and SPIONs@Au. (4) Hysterisis curves for SPIONs and SPIONs@Au at 5K before and after the purification. The value of saturation magnetization at 5 °K are 55 emu/g for SPIONs and for SPIONs@Au, after the modification of synthesis & purification process it changes from 38 to 58 emu/g. (5) Field Cooled (FC) and Zero Field Cooled (ZFC) curves for SPIONs@Au and SPIONs respectively. (6) Magnetic field generator, and the sample inserted into the copper coil. (7) Comparison of heat release with Fe_3O_4 and Fe_3O_4@Au at 44Hz frequency. (8) FT-IR comparison of surface functional groups in (a) Fe_3O_4 (b) Fe_3O_4@Au with that of (c) oleylamine & (d) oleic acid. (9) XPS data at Fe_{2p}, Au_{4f}, C_{1s} and O_{1s} edges for samples SPIONs and SPIONs@Au. (10) Binding energies (E_b) positions of Fe, Au, C, N, O for core and core-shell nanoparticles. (11) TGA analysis showing the weight loss as a function of temperature for SPIONs & SPIONs@Au.

[5] Some of the major advantages of iron oxide nanoparticles are. (1) They are biodegradable and biocompatible; [6] (2) Due to their intrinsic nano size, similar to that of biological entities, they can be easily incorporated within cells; either to modify the existing biological functions or to create new functions; [7] (3) Their unique properties can be fine tuned further by modifying their size, shape and composition; [8] (4) They can be made multifunctional; [9] (5) They can be bio-functionalized and hence can be targeted to specific biological tissue; [10] (6) They can be manipulated from a distance using magnetic fields; [11] and (7) They generate heat in the presence of oscillating magnetic fields, called hyperthermia.[12] Of these, hyperthermia using SPIONs has opened up a number of investigations for their application in cancer therapy. [13] It is now well established that local heat generation by using iron oxide nanoparticles for hyperthermia is capable of inducing tumor regression. [14], [15] Several different types of iron oxide nanoparticles have been examined for their effectiveness as hyperthermic agents. These can be classified into two major categories. The first category is superparamagnetic magnetite (Fe_3O_4) nanoparticles stabilized by a variety of ligands such as dextran, [16] cationic liposomes, [17] polyvinyl alcohol, hydrogel, [18] lauric acid [19] and maghemite (γ-Fe_2O_3) [18] nanoparticles stabilized by ligands such as dextran. [16] The second category is the ferrites such as cobalt ferrites ($CoFe_2O_4$), manganese ferrite ($MnFe_2O_4$), nickel ferrite ($NiFe_2O_4$), lithium ferrite ($Li_{0.5}Fe_{2.5}O_4$), mixed ferrites of nickel-zinc-copper ($Ni_{0.65}Zn_{0.35}Cu_{0.1}Fe_{1.9}O_4$) and cobalt-nickel ferrite ($Co_xNi_{1\_x}Fe_2O_4$). [19], [20] In addition to these superparamagnetic iron oxide nanoparticles, ferromagnetic nanoparticles such as Fe doped Au nanoparticles, Zn-Mn doped iron oxides ($Zn_xMn_{(1-x)}Fe_3O_4$) and Mn-Zn-Gd doped iron oxides ($Mn_xZn_xGd_xFe_{(2-x)}O_4$) composites [21] have also been examined for their hyperthermic activity. Very recently, extremely high heating performance such as 1300–1600 W/g has been reported using FeCo metallic nanoparticles. [22]

Some of the current challenges in the design of SPIONs utilized for hyperthermia are as follows. (1) The frequency of oscillating magnetic fields is very high; in the range of KHz and MHz. [16–21] (2) They have only been evaluated for hyperthermic treatment of tumors by directly injecting them into the tumor bed and hence may not be effective for treatment of other types of tumors located far inside the body. [23] (3) Majority of the investigations carried out so far did not utilize SPIONs with targeting ability. [24] (4) Their Specific Power Loss (SPL), which can be directly correlated to the hyperthermic effect, has not improved significantly by changing size, shape and composition. [25] (5) Even if SPL values of some of the SPION derivatives such as cobalt and manganese ferrite nanoparticles are significant, their oxidative instability and bio-incompatibility continues to be an issue. [26] The only clinical trial to date, utilizing magnetic nanoparticles for hyperthermia is that of SPIONs for the treatment of brain cancer. [27]

One possible approach to influence the hyperthermic effect of SPIONs is to provide a metallic shell around them as it has been well established that the magnetic properties of core nanomagnets change dramatically when encapsulated within a shell material. [28] For example, gold shell around iron oxide and cobalt nanoparticles changed the magnetic properties of the core magnetic material. [29], [30] We have been interested in biomedical applications of magnetic nanomaterials ranging from drug delivery to diagnosis. We have recently demonstrated the application of targeted SPIONs as contrast agents for MRI of tumors and their micrometastases [31] and potential application of oscillating magnetic fields for controlled drug delivery based on magnetic-polymer nanocomposites. [30], [32] Taking advantage of the possibility to generate heat locally using magnetic nanoparticles on application of oscillating magnetic field, we have recently initiated research to modulate the hyperthermic effect of iron oxide nanoparticles through incorporation of gold shell around the iron oxide core. Here in this report, we demonstrate a 4- to 5-fold increase in the amount of heat released with gold-coated SPIONs (SPIONs@Au; size: 6.3 nm), in comparison with

SPIONs (size: 5.4 nm), on application of low frequency oscillating magnetic fields (44 – 430 Hz). To the best of our knowledge this is the first report of enhanced hyperthermia using low frequency oscillating magnetic fields. Details of the influence of frequencies of oscillating magnetic field, concentration of the particles and media on the quantity of heat generated are also presented. We also show that, similar to SPIONs, SPIONs@Au do not elaborate much cytotoxic response in MCF-7 breast carcinoma cells and H9c2 cardiomyoblasts, the two representative mammalian cell types tested in culture.

EXPERIMENTAL

Synthesis of SPIONs@Au nanoparticles

Briefly, 0.71 g of iron acetylacetonate was mixed with 20 ml of phenyl ether, 2 ml of oleic acid and 2 ml of oleylamine under inert atmosphere with vigorous stirring. 2.58 g of 1,2 hexadecanediol was added to the solution. The solution was heated to around 210 °C with reflux for 2 h maintaining oxygen free conditions. The reaction mixture was cooled to room temperature and then ethanol (degassed) was added to precipitate the black colored product. The precipitate was separated out by centrifugation. The precipitated product was then washed with a series of solvents starting with hexane, followed by a mixture of hexane and ethanol and then finally with ethanol. The product was dispersed in ethanol and separated magnetically and dried to obtain a black colored powder which could be well dispersed in toluene. To 10 ml of phenyl ether, approximately 0.5 g of SPIONs was added. To this mixture, a solution containing 30 ml of phenyl ether, 3.1 g of 1,2-hexadecanediol, 0.5 ml of oleic acid, 3 ml of oleylamine and 0.83 g of gold acetate was added under inert atmosphere. The reaction mixture was heated to around 190 °C with reflux for about 1.5 h. After cooling to room temperature, ethanol was added and the dark purple material was separated out by centrifugation. The material was re-suspended in hexane, washed thrice with ethanol and dried. With the help of magnetic separation technique, by suspending the particles in ethanol, the magnetic gold-coated iron oxide nanoparticles were separated from the non magnetic gold nanoparticles and any unwanted carbon mass produced from oleic acid/ oleylamine used during the course of the reaction.

Characterization of SPIONs@Au nanoparticles

HRTEM analyses were carried out by using JEOL-2010 HRTEM instrument with a point to point resolution of 1.94 Å, operated at 200 kV accelerating voltage. The magnetic measurements were conducted using a Quantum Design MPMS-5S superconducting quantum interference device (SQUID) magnetometer. Small Angle X-ray Scattering (SAXS) measurements were carried out at the Center for Advanced Microstructures and Devices (CAMD) with synchrotron radiation of wavelength, $\lambda = 1.55$ Å. The SPIONs were dispersed in toluene and sealed in glass capillaries. The scattering pattern was imaged with a 2 dimensional Gabriel style multi-wire gas detector with a 200 mm active diameter and a resolution of 200–250 μm FWHM in a 1024 × 1024 array. The sample and the detector chamber were kept under vacuum during the measurements to maximize the intensity and to minimize the scattering from air. Scattering curves were monitored in a Q-range from 0.0066 to 0.164 $Å^{-1}$. Azimuthally averaged data from the detector were normalized for average transmitted intensity and corrected for background. X-ray Photoelectron Spectroscopy (XPS) analyses were done on AXIS 165 High Performance Multi-Technique Surface Analyzer which is based on a 165mm mean radius hemispherical analyzer, with an eight channeltron detection system. For UV-Visible spectroscopy, QE65000 spectrometer supplied by Ocean Optics limited was used and the samples were dispersed in toluene. The thermal stability of the samples was analyzed by using Thermogravimetric Analysis (TGA). Starting from room temperature, the samples were heated upto 600 °C at a rate of 10 °C per min on a TA 600 instrument.

Hyperthermia Measurements

The apparatus for determining the heat release utilizes a sinusoidal time-varying magnetic field generated at the center of a conductor coil by passing an alternating electric current (AC) through it (Figure S6). More details about the measurements and the apparatus can be found in our previous publications.[32] The Alternating Magnetic Field (AMF) induced heat release experiments were carried out by using a custom made setup with a power supply (P1351 Behlman AC power source) to control the magnetic field inside of a copper coil (Alpha-Core Inc.). The coil has an outer diameter of 6.75 inches and an inner diameter of 0.6875 inch. It was 0.5 inch thick and containing a total of 258 turns. Each experimental sample was placed inside the coil. The maximum parameters that can generate this field were a frequency of 430 Hz, 123 V at a current of 11 A and the lowest parameters are 44 Hz, 15 V at 11 A. A median frequency of 230 Hz, 67 V at 11 A also created the same field. These three frequencies 44, 230, and 430 Hz were used to study the effects of frequency on the heat release of iron oxide and iron oxide@Au during 60 min of exposure time. The data generated was arranged in a multivariate repeated measures fashion and analyzed using the PROC GLM in SAS software. The multivariate tests showed that there were highly significant effects of TIME, TIME*FREQUENCY, and TIME*TYPE OF MATERIAL* FREQUENCY when the heating efficiency data for SPIONs was compared with gold coated SPIONs.

Measurement Viability of H9c2 Cardiomyoblasts and MCF-7 Breast Carcinoma Cells Based on Metabolic Activity

Rat embryonic H9c2 cardiomyoblasts were maintained in Dulbecco's Modified Eagle's Medium (DMEM) containing 10% (v/v) fetal bovine serum (FBS) and 1% antibiotics (pencillin: 100 units/ml; streptomycin: 100 μg/ml) and incubated at 37 °C, 5% CO_2 and in 95% humidity. Approximately 50,000 cells/well were seeded onto 24-well plates. After 16 h incubation, the medium was replaced by 0.5 ml each of DMEM containing 2% (v/v) FBS and nanoparticles of either SPIONs or SPIONs@Au (concentration range: 25–500 μg/ml) and incubated for an additional 24 h. At the end of incubation, the metabolic activity of cells was assessed based the phenazine methoulfate (PMS)-assisted reduction of 3-(4,5-dimethylthiazol-2-yl)-5-(3-carboxymethoxyphenyl)-2-(4-sulfophenyl)-2H-tetrazolium (MTS) to MTS formazan. Briefly, aliquots (20 μl each) of the CellTiter 96 AQueous ™ reagent from Promega (Madison, WA) containing both PMS and MTS was added to the cell cultures and incubated for 3–4 h. The amount of MTS formazan produced during this time was measured at 490 nm using an ELx800 UV-Vis ELISA plate reader (BioTek Instruments). The percentage cell viability was calculated with respect to the control, untreated cells (set at 100%). The values shown are mean ± SD of three experiments. [33]

The MCF-7 breast carcinoma cells were maintained in Eagle’s Minimum Essential Medium (EMEM) containing 0.01mg/ml bovine insulin, 10% (v/v) FBS and 1% (v/v) antibiotics (penicillin: 100 units/ml; streptomycin: 100 μg/ml) and incubated at 37 °C, 5% CO_2 and in 95% humidity. Approximately, 50,000 cells were exposed to either SPIONs or SPIONs@Au (25–500 μg/ml) for 24 h and the cell viability based on metabolic activity (i.e., MTS reduction; discussed above) was determined using the CellTiter 96 AQueous ™reagent (see above). Similar to H9c2 cardiomyoblasts, the changes in cell viability of MCF-7 cells was calculated with reference to the corresponding untreated control cells (set at 100%).

RESULTS AND DISCUSSION

For the synthesis of iron oxide (Fe_3O_4) and gold-coated iron oxide (Fe_3O_4@Au), we have modified the procedure described previously. [34] The synthesized SPIONs and SPIONs@Au nanoparticles were characterized by different instrumental techniques such as

HRTEM, FT-IR, UV-Vis, XPS, SAXS, SQUID (see, Supporting Information). The SPIONs@Au shell particles, which are responsive to magnets, were purified by first treating with hexane, followed by a mixture of hexane and ethanol and finally ethanol. With the help of magnetic separation technique, by suspending the particles in ethanol, we have separated only the gold-coated iron oxide material leaving non magnetic gold nanoparticles and any unwanted carbon mass produced from oleic acid/oleylamine during the course of the reaction.

The HRTEM measurements show their spherical nature and the sizes of SPIONs and SPIONs@Au are 5.4 ± 0.4 nm and 6.3 ± 0.7 nm respectively (Figure 1 and Figure S1). The particles are well dispersible in toluene and their UV-visible absorption spectra showed a clear surface plasmon resonance (SPR) band at 558 nm; which is the characteristic optical property of gold nanostructures confirming that the core Fe_3O_4 is coated with Au shell (Figure S2). Small angle-x-ray scattering analysis was carried out using CAMD's synchrotron beam line (www.camd.lsu.edu). Figure-2 shows the SAXS data for both the non-coated and coated nanoparticles. The mean particle diameters determined from the SAXS data were 4.6 ± 0.4 and 5.3 ± 0.4 nm for the SPIONs and SPIONs@Au respectively (Figure S3). [35] From both HRTEM and SAXS data, the observed difference in the diameter between coated and non-coated samples suggests the formation of a gold coating of approximately 0.4 to 0.5 nm thick. (Note that the atomic diameter of gold is 0.288 nm and the observed difference in the size of SPIONs and SPIONs@Au corresponds to approximately twice this value as expected.)

Magnetic characterization of the samples was carried out with a superconducting quantum interference device (SQUID) magnetometer. Based on the SQUID measurements, it can be seen from the hysteresis curves for SPIONs and SPIONs@Au at 5 K and 300K that no coercivity or remnance existed, indicating the superparamagnetic behavior of SPIONs before and after coating with gold (Figure S4). The saturation magnetization (M_s) of SPIONs@Au increased slightly on coating with gold (M_s values for SPIONs & SPIONs@Au nanoparticles is 55 emu/g and 58 emu/g respectively). Compared to previously published results where the M_s of SPIONs@Au is much smaller than that of SPIONs, our results show that the saturation magnetization (M_s) changes from 38 to 58 emu/g on further purification (Figure S4). [34] Both zero field cooled (ZFC) and field cooled (FC) temperature dependent magnetization curves for SPIONs and SPIONs@Au show that the blocking temperature more than doubles on gold coating (Figure S5: T_b for SPIONs and SPIONs@Au is 19.1 K and 44.3 K respectively). Most of the published literature suggests that upon forming a layer around magnetite nanoparticles with biocompatible metal or polymer, there is generally a decrease in the magnetization values. [34], [36] However, in the present case, the SPIONs@Au have much higher magnetization values than those reported in the literature and we believe that careful purification of the sample to make it free from unwanted pure gold nanoparticles is responsible for the result.

Hyperthermia of SPIONs@Au - Changes in Temperature of the Medium

The temperature increase with time for SPIONs and SPIONs@Au in water on application of oscillating magnetic field is shown in Figure 3. Both the samples were excited with a 44Hz frequency at 465 Oe magnetic fields. The temperature raise and the time required to reach therapeutic temperature (42 °C) was faster for SPIONs@Au compared to SPIONs. Also, there is a 4- to 5-fold difference in the temperature obtained between the gold-coated and free SPIONs at the same level of concentration based on pure iron oxide after subtracting the weight of ligand and gold shell (Figure S7). This feature of high heat power generated per particle is particularly important for applications where the target concentration is very low as for instance in antibody targeting of tumors. [37] One can also see an increase in heat release with time up to 30 min followed by a reduction with further exposure. The heat

release is also frequency dependent and within a range of 44 Hz to 430 Hz, highest release is seen at 44 Hz (Figure 4A). Another interesting observation is that the heat release increases with concentration in case of SPIONs and the opposite is observed in case of gold-coated SPIONs pointing to a possible quenching of heat as gold is a better conductor (Figure 4B). The heat generation also appears to be dependent on Brownian-rotation loss mechanism in addition to the Neel relaxation as we see a dependence on the nature of the medium. Figure 5 shows the heat release measurements with different media to determine the influence of media on the hyperthermia of SPIONs@Au. Even though the particles are hydrophobic and well dispersed in toluene compared to water, the heat release is 2- to 3-fold higher in water compared to toluene.

Hyperthermia of SPIONs@Au - Specific Power Losses (SPL)

The heat release can also be determined based on the Specific Power Losses (SPL also called Specific Power Absorption, SPA). SPL is defined as the capability to generate heat from the magnetic coupling between the magnetic moment of nanoparticles and the applied oscillating magnetic field. SPL for a number of magnetic nanoparticles and different types of SPIONs has been reported in the literature were calculated by using the following equation,

$$\mathrm{SPL}=\frac{\mathrm{CV_s}}{\mathrm{M}}\frac{\mathrm{dT}}{\mathrm{dt}}$$

Where C is the specific heat of the sample (C = 4.185, 2.44, and 1.13 J/g/°C for water, ethanol, and toluene, respectively), Vs is the volume of the sample medium, M is the weight of the magnetic material, and dT/dt is the raise in temperature per unit time.

In order to evaluate the effect of gold shell on the heat release process, we have determined the SPL of free SPIONs and gold-coated SPIONs. The calculated average of SPL values for three different concentrations of SPIONs and SPIONs@Au at the corresponding frequencies are as follows (Figure 6 and Table-1). For SPIONs, the SPL values are 256.81 W/g (at 44Hz), 249.8 W/g (230 Hz) and 313.5 W/g (430 Hz); similarly for Fe_3O_4@Au, the values are 444.32 W/g (44 Hz), 317.75 W/g (230 Hz) and 463.9 W/g (430 Hz). For both SPIONs & SPIONs@Au, there is a decrease in SPL value at 230Hz frequency compared to other two. For gold-coated SPIONs, the highest temperature raise (49 °C) was found at 44 Hz, whereas the highest SPL value (463.9 W/g) was observed at 430 Hz.

The influence of solvent on SPL is noteworthy as seen from Figure-7. The figure shows comparison of SPL values for Fe_3O_4@Au (1.0 mg concentration) at 44Hz, 230Hz and 430Hz frequencies in water, ethanol and toluene medium. At 44Hz, the gold-coated SPIONs show highest temperature increase in water medium (49 °C) compared to ethanol and toluene. However, the SPL dependency of SPIONs@Au on solvent is also influenced by the frequency of the oscillating magnetic field with the highest value of 976W/g in ethanol at 430Hz frequency (920.7W/g for water and 113 W/g for toluene). While at 44 Hz, the SPL value in water medium is highest (648.6 W/g) compared to ethanol (431W/g) and toluene (86.6 W/g). The SPL values at 230Hz frequency are in the order of 325.5 W/g for water, 374.1 W/g for ethanol and again 86.6 W/g in toluene (Table-2). Similar to temperature increase, what is really surprising is the dramatic drop in heat release as determined from SPL values in toluene even though the particles are compatible with toluene rather than with hydrophilic medium such as water and ethanol. One possible explanation for this is likely the rate of heat dissipation which is anticipated to be highest in toluene as the particles disperse well in that medium. Another possible explanation is the viscosity differences between toluene and water/ethanol. The lower viscosity of toluene (0.68 mPa.s. *vs* 1.0

mPa.s. for water and 1.1 mPa.s. for ethanol) is likely be enhancing the Brownian fluctuation of the particles thereby reducing the heat release. This is supported by a recent report suggesting that the frictional mechanism contributes to SPL. [22] In addition, low specific heat rate of toluene could also be a contributing factor. However, the reason for differences in heat release between ethanol and water medium is not clear at this point. From the frequency dependent measurements between SPIONs & SPIONs@Au and the solvent dependent measurements of SPIONs@Au, one can draw a conclusion that overall the SPL is both frequency and solvent dependent. In ethanol medium, it is more at highest frequency of 430Hz and whereas in water medium, SPL is maximum at lowest frequency of 44Hz.

What we have demonstrated experimentally is the fact that the hyperthermic effect of SPIONs enhances dramatically on coating with Au. While we cannot explain completely the reason for such an enhancement, we could advance possible reasoning based on the fact that gold coated SPIONs retain their superparamagnetic fraction much better compared to SPIONs alone. [38] The Néel relaxation time, T_N, of the magnetic nanoparticles under an external magnetic field is expressed by following formula:

$$\mathrm{T_N} = \frac{\sqrt{\pi}}{2}\mathrm{T_0}\frac{\mathrm{Exp}(\mathrm{KV_m}/\mathrm{K_B T})}{(\mathrm{KV_m}/\mathrm{K_B T})^{1/2}}$$

where T_0 is the relaxation time constant and has the order of 10^{-9} s, K is the anisotropy constant, and V_M is the magnetic volume of particles. The Néel relaxation time, T_N, is therefore can be determined as the ratio of the energy of magnetic anisotropy of superparamagnetic particles to the thermal energy. One possible reason enhanced hyperthermic effect on gold coating is the ability of gold coating to retain the superparamagnetic fraction of the SPIONs much better compared to SPIONs alone [38] leading to higher energy of magnetic anisotropy of superparamagnetic particles within the gold shell compared to the naked SPIONs. One could also speculate that the higher heat capacity of the gold shell to shield the heat generated within the SPIONs could be responsible for enhancing the temperature raise on application of oscillating magnetic field.

Hyperthermia of SPIONs@Au - Evaluation of Cytotoxicity

In order for application of gold coated SPIONs for thermolysis of cancer cells, it is important to demonstrate that they are not cytotoxic. Therefore, the cyctotoxicity of SPIONs@Au was compared with SPIONs. The cell viability of SPIONs and SPIONs@Au with different concentrations was quantitatively estimated to explore the feasibility of utilizing SPIONs@Au nanoparticles for targeted cancer therapy. The studies performed using H9c2 cardiomyoblasts (Figure 8(a)), a non-cancerous stable cell line derived from embryonic rat heart and known to express specific cardiac markers (considered a close proxy for adult cardiac cells), indicate that both SPIONs and SPIONs@Au are inherently least cytotoxic upto 250 μg/ml concentration and for 500 μg/ml, a 20% reduction in cell viability was observed when studied in the absence of oscillating magnetic field. Similar results were obtained when MCF-7 breast carcinoma cells were exposed to either SPIONs or SPIONs@Au in the concentration range of 25 to 250 μg/ml and with a 500 μg/ml concentration, a 20–30% reduction in viability for 24 h, i.e., in the absence of oscillatory magnetic field (Figure 8(b)). The maximum decrease in viability of cells at the highest concentration of 500 μg/ml concentration: for H9c2 cell line, SPIONs-18% and SPIONs@Au-14%. For MCF7 cell line at the same concentration, SPIONs-30%, SPIONs@Au-23%.

There have been some studies in the literature that showed that maghemite (Fe_2O_3) nanoparticles are cytotoxic to different cell types. [39], [40] In most cases the nanoparticles employed in these studies did not have a biocompatible or protective coating that could possibly prevent the seepage of Fe into the cellular milieu. Support for this notion comes from the fact that, in general, the cytotoxicity of iron oxide nanoparticles appears to be consequence of Fe-induced intracellular formation of reactive oxygen species, ROS. The SPIONs and SPIONs@Au we described are comparatively smaller in size than those reported by others. [40] Also, our SPIONs and SPIONs@Au contain oleic acid and oleylamine as codispersants. Both these dispersants contain a single carbon-carbon double bond at C9–10 position. Therefore, it is possible that these agents, apart from preventing the agglomeration, can impart significant protection against Fe-mediated toxicity if any. [41] We determined the cytotoxicity in two different cell lines, namely, MCF-7 carcinoma cells and H9c2 cardiomyoblasts at a range of concentrations of SPIONs and SPIONs@Au (25–500 μg/ml) (Fig. 8). We are aware that some of the concentrations used here are way more than physiological concentrations. However, the concentrations are based on the total weight of the sample including the ligand and not just the weight of the Fe. Many publications report cell viability w.r.t. to weight of Fe. In our case the percentage of Fe in SPIONs and SPIONs@Au is only 14.5 % and 11.1 % respectively (from elemental analysis). In any case, we chose to test this wide range of concentrations firstly to establish their limits of tolerance by the two cell lines used. Also, it is our contention that if there is scope for Fe-mediated toxicity, it should be expressed, at least, in part, irrespective of the uptake of SPIONs and SPIONs@Au added to these cultures. For instance, if the particles reside predominantly outside the cells and release Fe, there should be substantial expression of cytotoxicity either by the uptake of Fe released into the medium or Fe-dependent oxidation of serum components that could result in the accumulation of ROS and subsequent interaction with the cells in culture. Similarly, if the SPIONs and SPIONs@Au are taken up by the two cell lines and release Fe inside the cells, there again should be expression of toxicity reflected in altered red-ox metabolism of cells. Our studies show that the cytotoxicity measured in terms of MTS reduction is not significantly different for the SPIONs and SPIONs@Au in both MCF-7 carcinoma cells and H9c2 cardiomyoblasts (Fig. 8). Further, within a given cell type, there appears to be a tendency toward increased cytotoxicity at higher concentrations of either SPIONs or SPIONs@Au. For example, at the highest concentration of 500 μg/ml employed in the assay, there was no more than 20% reduction in cell viability in H9c2 cardiomyoblasts. Similarly, with MCF-7 carcinoma cells, the reduction in the level of cell viability at 500 μg/ml was around 30% or less for SPIONs and SPIONs@Au. Although the results presented here are only with two cells, one non-cancerous (H9c2 cardiomyoblasts) and the cancerous (MCF-7 carcinoma cells), it appears that the SPIONs and SPIONs@Au we prepared are inherently less cytotoxic to mammalian cells in culture. We do not know the reasons for this low cytotoxicity, although it is tempting to speculate that oleic acid-oleylamine co-dispersants may be responsible for part of the protection. [41] Another possible reason is that the cytotoxicity assay based on red-ox metabolism of viable cells might not be sensitive enough to pick up subtle changes that could eventually lead to cell death. Our results are also supported by recent studies that demonstrate similar lack of cytotoxicity of SPIONs [42] as well as gold coated iron oxide nanoparticles. [43] More detailed studies are currently underway to determine the extent of uptake of SPIONs and SPIONs@Au by H9c2, MCF-7 and other cancerous and non-cancerous cells and also to examine the affect of oscillatory magnetic field on the fate of cells loaded with SPIONs, SPIONs@Au, and SPIONs@Au tagged with luteinizing hormone-releasing hormone and/or folic acid.

CONCLUSION

In conclusion, we report promising magnetic nanoparticles, SPIONs@Au that have suitable chemical, physiological, physical and biological properties for magnetic hyperthermia applications in low frequency oscillating magnetic field (<500 Hz). While the published literature demonstrate magnetic nanoparticle hyperthermia in the presence of oscillating magnetic fields ranging from KHz to MHz, our results indicate possibilities for utilization very low frequency oscillating magnetic fields in hyperthermia treatment. Also, the differences in heat release between SPIONs@Au and SPIONs is at first intriguing and investigations are underway to understand the reasons. It is well established that the heat generation is a result of a combination of internal Néel fluctuations of the particle magnetic moment, hysteresis and to the external Brownian fluctuations that all rely on the magnetic properties of nanoparticles. It has been recently reported that Fe nanoparticles show dramatically higher heat generation compared to iron oxide nanoparticles due to their greater magnetization and hysteresis. [44] Even though there are no major differences in magnetic properties of SPIONs and SPIONs@Au, one possible explanation is the ability of gold coating to retain the superparamagnetic fraction of the SPIONs much better compared to SPIONs alone leading to higher energy of magnetic anisotropy of superparamagnetic particles within the gold shell compared to the naked SPIONs. One could also speculate that the higher heat capacity of the gold shell to shield the heat generated within the SPIONs could be responsible for enhancing the temperature raise on application of oscillating magnetic field. Nevertheless, the hyperthermia of SPIONs@Au described in this report represent a new generation of multifunctional magnetic nanoparticles which can provide a combination of diagnostic and therapeutic tools. Gold nanoshell have been shown to be excellent candidates for the diagnosis and therapy through a variety of mechanisms. [45] In addition, the gold nanoshell offers opportunities for biofunctionalization thereby providing targeting ability for hyperthermia based on SPIONs@Au nanoparticles. Excellent hyperthermia exhibited by SPIONs@Au nanoparticles coupled with their lack of cytotoxicity is anticipated to make them into suitable candidates for thermolysis of cancer cells. [46]

Supplementary Material

Refer to Web version on PubMed Central for supplementary material.

Acknowledgments

We thank Louisiana Board of Regents for an equipment grant to purchase SQUID magnetometer (LEQSF (2008–10)-ENH-TR-07). FM thanks CAMD for the opportunity to carry out his thesis work in CAMD's nanomaterials and nanofabrication facility. Partial funding for this work from DOE Energy Frontier Research Center (Grant No. DE-SC0001058) and NIH (1R01CA142842-01A1) is gratefully acknowledged.

REFERENCES

1. (a) Wilhelm C, Gazeau F. Biomaterials. 2008; 29:3161–3174. [PubMed: 18455232] (b) Lee J-H, Schneider B, Jordan EK, Liu W, Frank JA. Adv. Mater. 2008; 20:2512–2516. [PubMed: 19578472]
2. (a) Sebastianelli A, Sen T, Bruce I. Lett. Appl. Microbiol. 2008; 46:488–491. [PubMed: 18346135] (b) Smith JE, Wang L, Tan W. Trends Anal. Chem. 2006; 25:848–855.
3. (a) Yang L, Ren X, Tang F, Zhang L. Biosens. Bioelectron. 2009; 25:889–895. [PubMed: 19781932] (b) Kumar, Challa, editor. Nanomaterials for Biosensors. Weinheim, Germany: Wiley-VCH; 2007.
4. (a) Yu Y, Sun D. Expert Rev. Clin. Pharmacol. 2010; 3:117–130. [PubMed: 22111537] (b) Kumar, Challa, editor. Nanomaterials for Medical Diagnosis and Therapy. Weinheim, Germany: Wiley-VCH; 2007.

5. Dilnawaz F, Singh A, Mohanty C, Sahoo SK. Biomaterials. 2010; 31:3694–3706. [PubMed: 20144478]
6. (a1) Sanvicens N, Marco P. Trends Biotechnol. 2008; 26:425–433. [PubMed: 18514941] (b) Jain T, Reddy M, Morales M. Mol. Pharm. 2008; 5:316–327. [PubMed: 18217714]
7. (a) Corchero J, Villaverde A. Trends Biotechnol. 2009; 27:468–476. [PubMed: 19564057] (b) Purushotham S, Chang P, Rumpel H. Nanotechnology. 2009; 20:305101. [Epub 2009 Jul 7; doi: 10.1088/0957-4484/20/30/305101]. [PubMed: 19581698]
8. Kumar, Challa, editor. Magnetic Nanomaterials for Life Sciences. Weinheim, Germany: Wiley-VCH; 2009.
9. (a) Mornet S, Vasseur S, Grasset F, Duguet E. J. Mater. Chem. 2004; 14:2161–2175.(b) Pathak P, Katiyar VK. Azonano. 2007; 3:1–17. [doi: 10.2240/azojono0114].
10. (a) Kumar, Challa, editor. Nanomaterials for Cancer Diagnosis. Weinheim, Germany: Wiley-VCH; 2007. (b) Kumar, Challa, editor. Nanomaterials for Cancer Therapy. Weinheim, Germany: Wiley-VCH; 2007.
11. (a) Derfus A, Maltzahn G, Harris T. Adv. Mater. 2007; 19:3932–3936.(b) Wilhelm C, Gazeau F. J. Magn. Magn. Mater. 2009; 321:671–674.
12. (a) Thiesen B, Jordan A. Int. J. Hyperther. 2008; 24:467–474.(b) Zee V. Ann. Oncol. 2002; 13:1173–1184. [PubMed: 12181239]
13. Zhang Z, Mascheri N, Dharmakumar R, Li D. Cytotherapy. 2008; 10:575–586. [PubMed: 18608350]
14. Bao F, Yao J-L, Gu R-A. Langmuir. 2009; 25:10782–10787. [PubMed: 19552373]
15. (a) Kowal CD, Berino JR. Cancer Res. 1979; 39:2285–2289. [PubMed: 376118] (b) Habash R, Bansal R, Krewski D, Alhafid H. Crit. Rev. Biomed. Eng. 2006; 34:491–542. [PubMed: 17725480]
16. Dennis CL, Jackson AJ, Borchers JA, Ivkov R. J. Phys. D: Appl. Phys. 2008; 41:1304020. [doi: 10.1088/0022-3727/41/13/134020].
17. Kawai N, Futakuchi M, Yoshida T. The Prostate. 2008; 68:784–792. [PubMed: 18302228]
18. (a) Makoto S, Yasutake H, Hiroaki M. J. Magn. Magn. Mater. 2009; 321:1493–1496.(b) Levy M, Wilhelm C, Jean S, Horner O. J. Phys: Condens. Matter. 2008; 20:204133. [doi: 10.1088/0953-8984/20/20/204133]. [PubMed: 21694262]
19. (a) Pradhan P, Giri J, Samanta G, Sarma DH, Mishra PK, et al. J. Biomed. Mater. Res. Part B: Appl. Biomater. 2006; 81:12–22. [PubMed: 16924619] (b) Seongtae B, Sang WL, Takemura Y. IEEE T. Magn. 2006; 42:3566–3568.
20. Dong-Hyun K, Se-Ho L, Kyoung-Nam K. J. Magn. Magn. Mater. 2005; 293:320–327.
21. (a) Andy W, Katherine AB, Joshua DA, Kimberly H-S. J. Magn. Magn. Mater. 2007; 309:15–19. (b) Sharma R, Chen CJ. J. Nanopart. Res. 2009; 11:671–689.
22. Nojima H, Ge S, Katayama Y, Ueno S, Iramina K. J. Appl. Phys. 2010; 107:09B320. [doi: 10.1063/1.3357987].
23. (a) Ito A, Honda H, Kobayashi T. Cancer Immunol. Immunother. 2006; 55:320–328. [PubMed: 16133113] (b) Shinkai M. J. Biosci. Bioeng. 2002; 94:606–613. [PubMed: 16233357]
24. Boehm FJ, Chen A. Recent Patents on Biomedical Engineering. 2009; 2:110–120.
25. Mornet S. Prog. Solid State Chem. 2006; 34:237–247.
26. (a) Fortin J-P, Gazeau F, Wilhelm C. Eur. Biophys. J. 2008; 37:223–228. [PubMed: 17641885] (b) Zeisberger M, Dutz S, Müller R. J. Magn. Magn. Mater. 2006 [doi:10.1016/j.jmmm/2006.11.178]. (c) Hütten A, Sudfeld D, Ennen I. J. Magn. Magn. Mater. 2005; 293:93–101.
27. Jordan A, Wust P, Fahling H, John W, Hinz A, Felix R. Int. J. Hyperther. 2009; 25:499–511.
28. Hormes J, Modrow H, Bonnemann H, Kumar C. J. Appl. Phys. Lett. 2005; 97:10R102–10R106.
29. Wang L, Park H-Y, Lim Stephanie I-I. J. Mater. Chem. 2008; 18:2629–2635.
30. Lu Z, Prouty M, Gao Z, Golub V, Kumar C. Langmuir. 2005; 21:2042–2050. [PubMed: 15723509]
31. Branca T, Cleveland ZI, Leuschner C, Kumar C, Fubara B, Maronpot RR, Warren W, Driehuys B. Proc. Natl. Acad. Sci. 2010; 107:3693–3697. [PubMed: 20142483]
32. Urbina M, Zinoveva S, Miller T, Sabliov C. J. Phys. Chem. C. 2008; 112:11102–11108.

33. (a) Sathishkumar K, Xi X, Martin R, Uppu RM. J. Alzheimer's Dis. 2007; 11:1261–1274.(b) Sathishkumar K, Haque M, Perumal TE, Francis J, Uppu RM. FEBS Lett. 2005; 579:6444–6450. [PubMed: 16288747]
34. Wang L, Luo J, Fan Q, Suzuki M. J. Phys. Chem. B. 2005; 109:21593–21601. [PubMed: 16853803]
35. Bonini M, Fratini E, Baglioni P. Mater. Sci. Eng. C. 2007; 27:1377–1381.
36. (a) Polina GR, Elena KB, Alexander GM, Nikolai VZ. Mendeleev Commun. 2010; 20:158–160.(b) Lingyan W, Jin L, Quan F, Masatsugu S, Itsuko S, Engelhard MH, Yuehe L, Nam K, Jian QW, Zhoung ChJJ. Phys. Chem. 2005; 109:21593.
37. Suzuki M, Shinkai M, Kamihira M. Biotechnol. Appl. Biochem. 1995; 2:1179.
38. Mikhaylova M, Kim DK, Bobrysheva N, Osmolowsky M, Semenov V, Tsakalakos T, Muhammed M. Langmuir. 2004; 20:2472–2477. [PubMed: 15835712]
39. Adopa LP, Qian Y, Shao R, Guo LN, et al. Part. Fibre Toxicol. 2009; 6:1–14. [PubMed: 19134195]
40. Pisanic, Thomas R., II; Blackwell, Jennifer D.; Shubayev, Veronica I.; Fiñones, Rita R.; Jin, Sungho. Biomaterials. 2007; 28:2572–2581. [PubMed: 17320946]
41. (a) Isabelle B, Shinkai A, Hiroyuki MH, Takeshi K. Cytotechnology. 1997; 25:231–234. [PubMed: 22358897] (b) Cury-Boaventura MF, Pompéia C, Curi R. Nutrition. 2005; 21:395–405. [PubMed: 15797684] (c)http://www.buzzle.com/articles/oleic-acid.html
42. (a) Hofmann A, Thierbach S, Semisch A, Hartwig A, Taupitz M, Ruehl E, Graf C. J. Mater. Chem. 2010; 20(36):7842–7853.(b) Park J, Yu MK, Jeong YY, Kim JW, Lee K, Phan VN, Jon S. J. Mater. Chem. 2009; 19(35):6412–6417.
43. Jafari T, Simchi A, Khakpash N. J. Colloid Interface Sci. 2010; (1):64–71. 345 1. [PubMed: 20153479]
44. Hadjipanayis C, Bonder M, Balakrishnan S, Wang X, Mao H, Hadjipanayis G. Small. 2008; 4:1925–1929. [PubMed: 18752211]
45. (a) Erickson, TA.; Tunnell, JW. Gold nanoshells in biomedical applications. In: Kumar, Challa, editor. Nanomaterials for the Life Sciences. Vol. 3. Weinheim, Germany: Wiley-VCH; 2008. p. 1-44.(b) Hirsch, LR.; Drezek, RA.; Halas, NJ.; West, JL. Diagnostic and therapeutic applications of metal nanoshells. In: Mauro, Ferrari, editor. BioMEMS and Biomedical Nanotechnology. Vol. 3. Springer; 2006. p. 157-169.
46. Yang X, Mahmood M, Fejleh A, Li Z, Watanabe F, Trigwell S, Little RB, Kunets VP, Dervishi E, Biris AR, Salamo GJ, Biris AS. Int. J. Nano Medicine. 2010; 5:167–176.

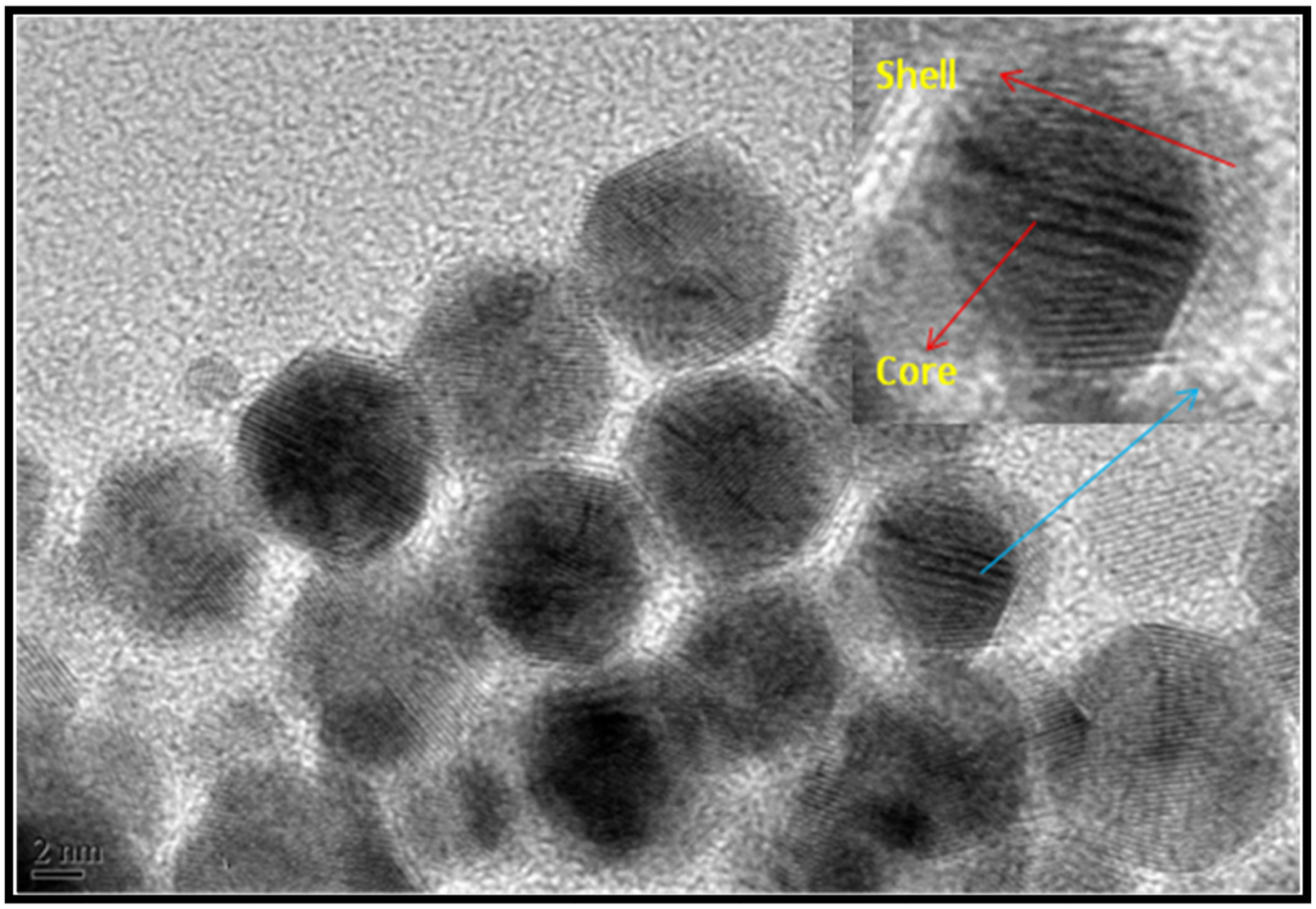

Figure 1.
HRTEM image of SPIONs@Au nanoparticles (inset showing the core and shell).

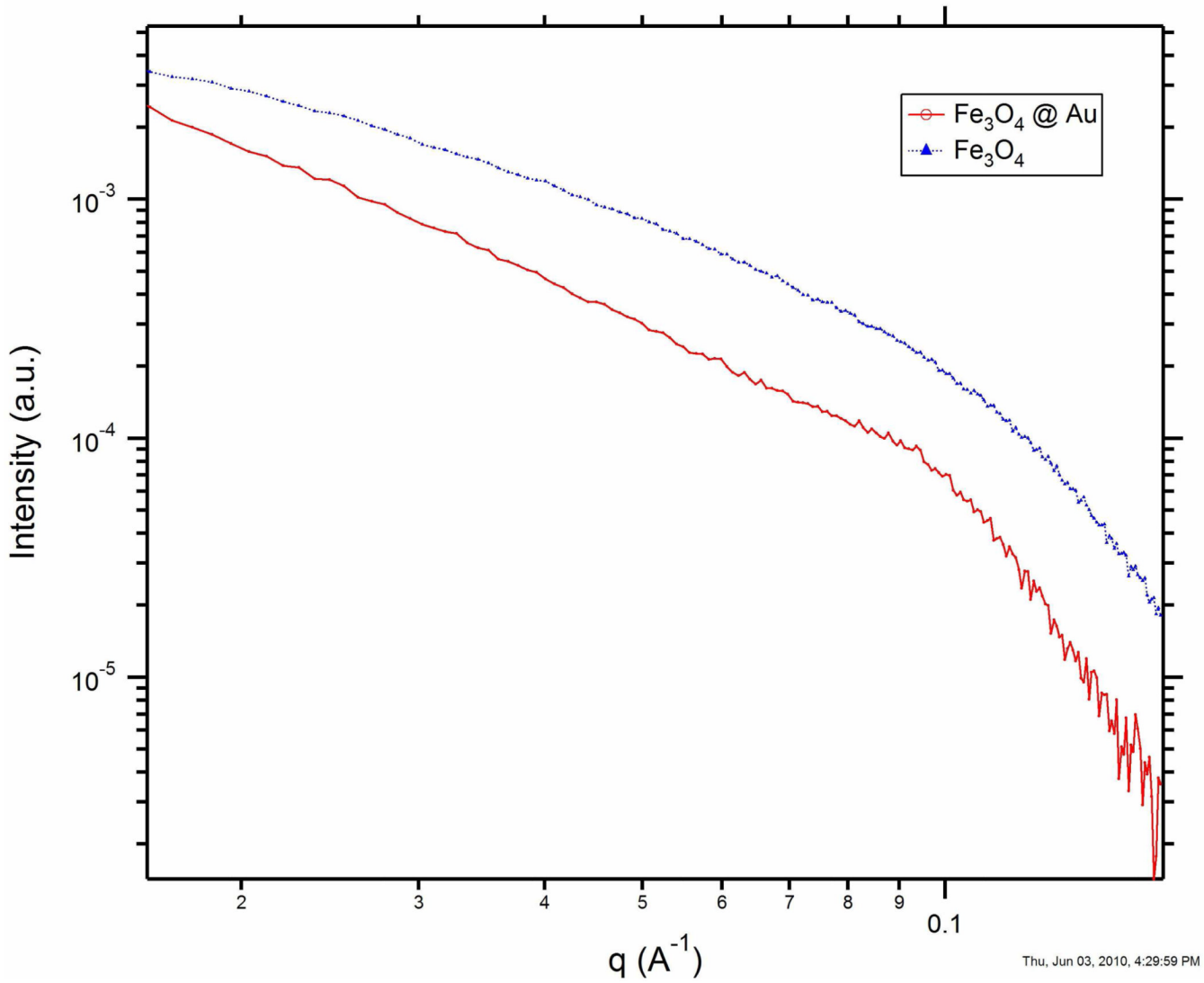

Figure 2.
SAXS for SPIONs and SPIONs@Au.

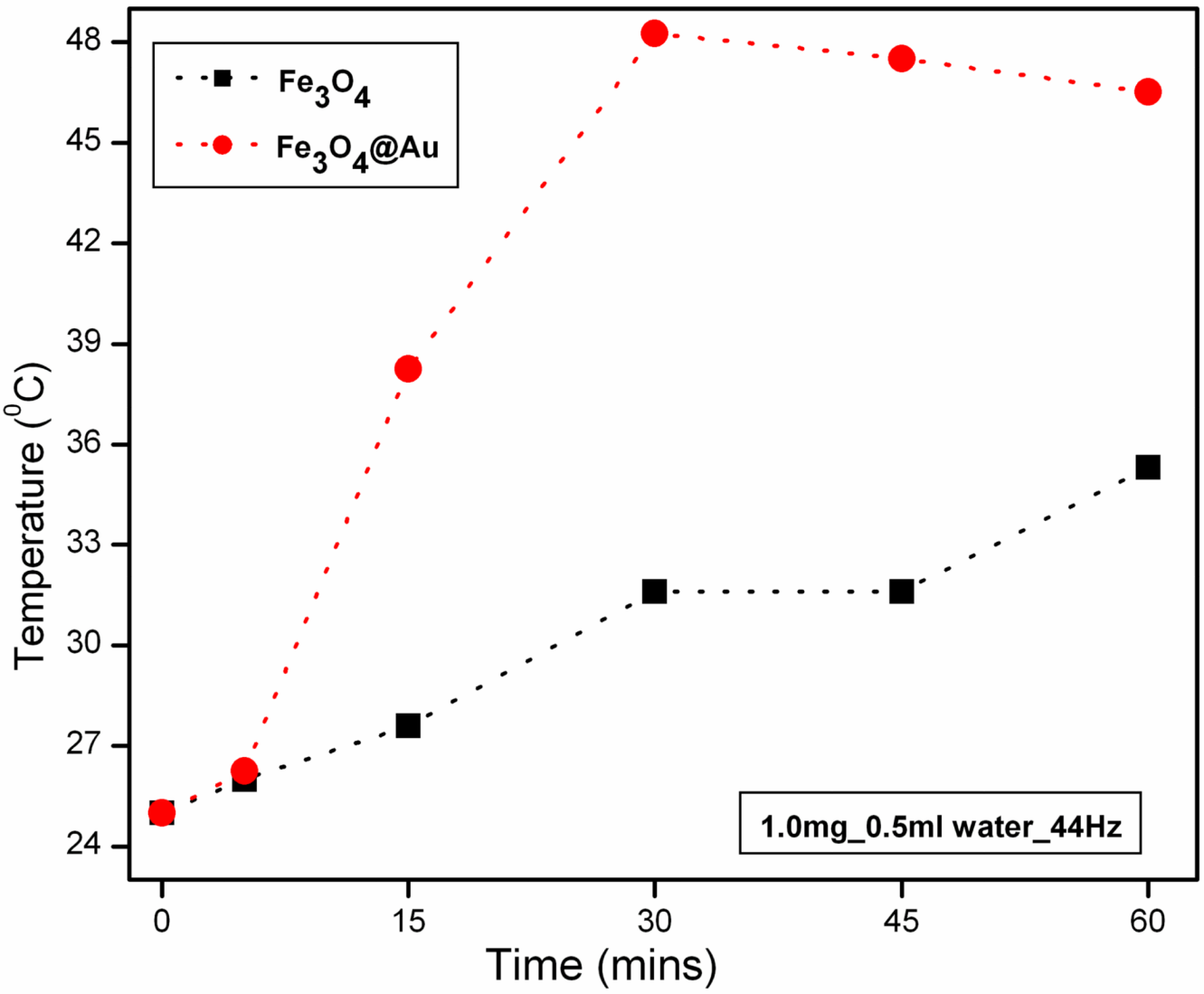

Figure 3.
Temperature versus time graphs for SPIONs and SPIONs@Au at a concentration of 1.0 mg/ 0.5 ml.

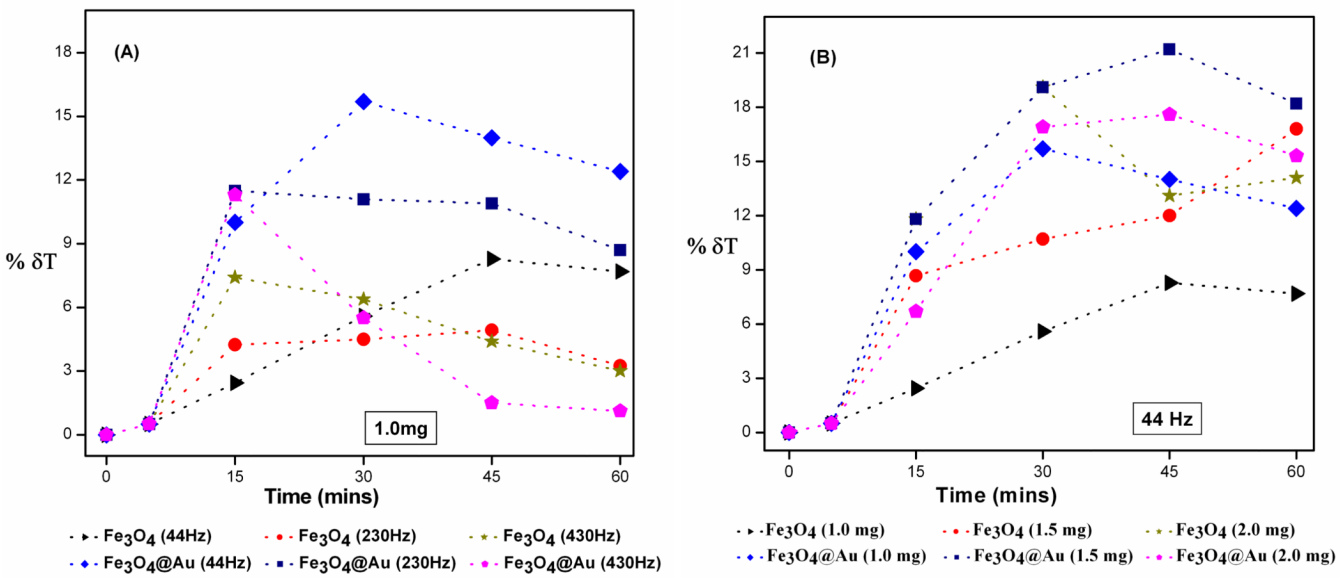

Figure 4.

(A) Comparison of heat release for SPIONs and SPIONs@Au at 44 Hz, 230 Hz, and 430 Hz (B) Comparison of heat release for SPIONs and SPIONs@Au at three different concentrations.

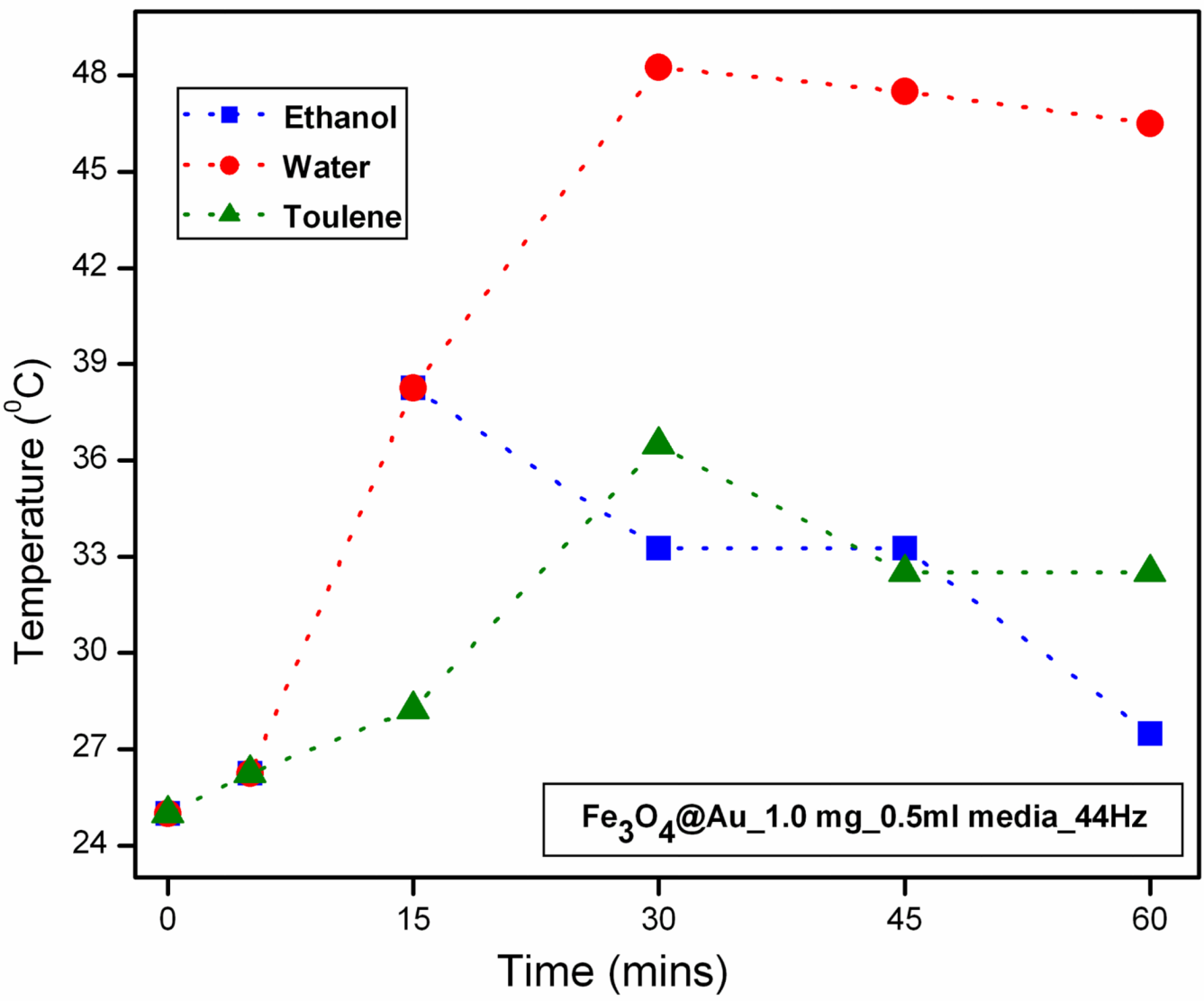

Figure 5.
Comparison of heat release by SPIONs@Au at 44 Hz in different solvents.

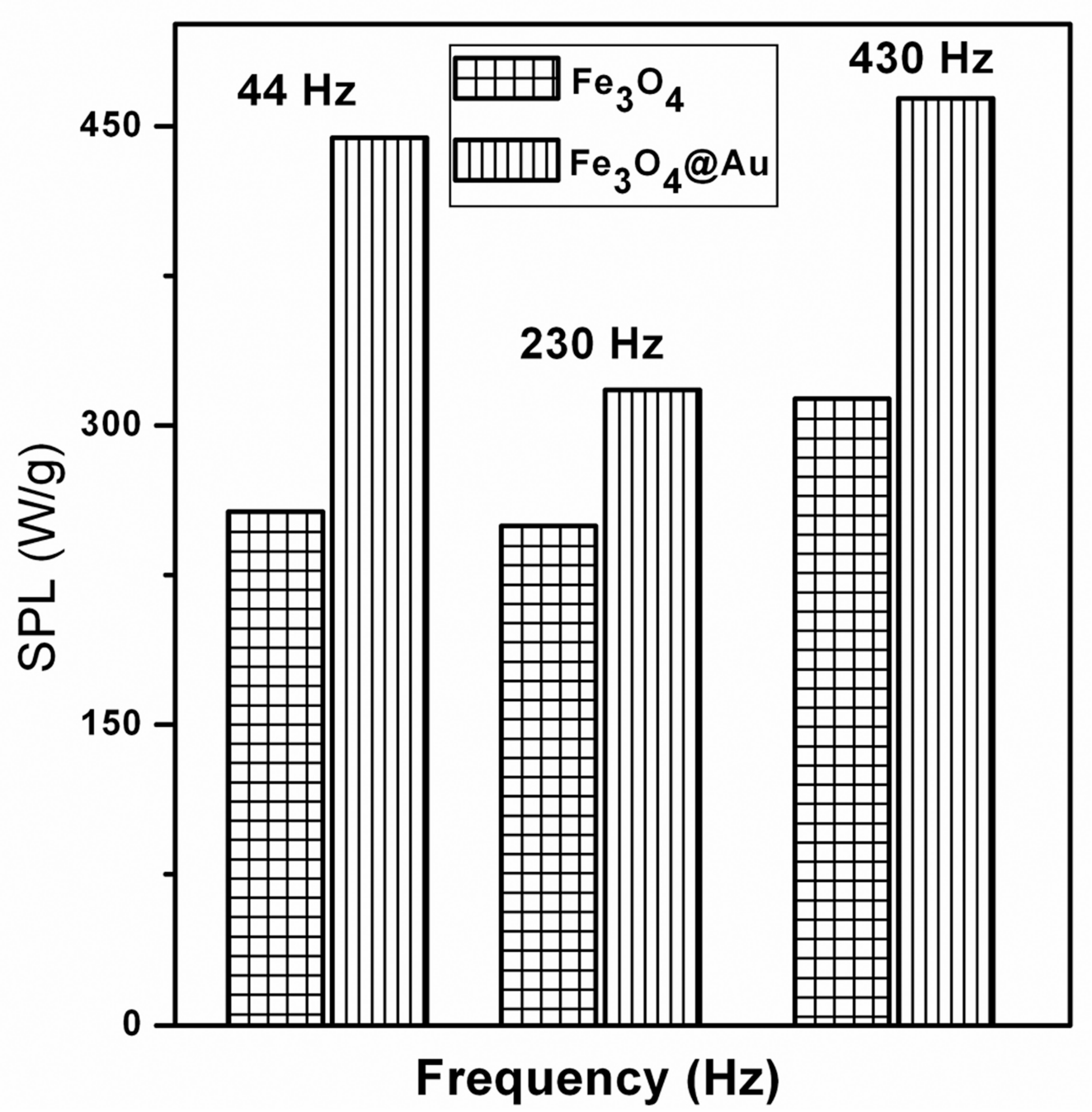

Figure 6.
Frequency dependent SPL values for SPIONs and SPIONs@Au

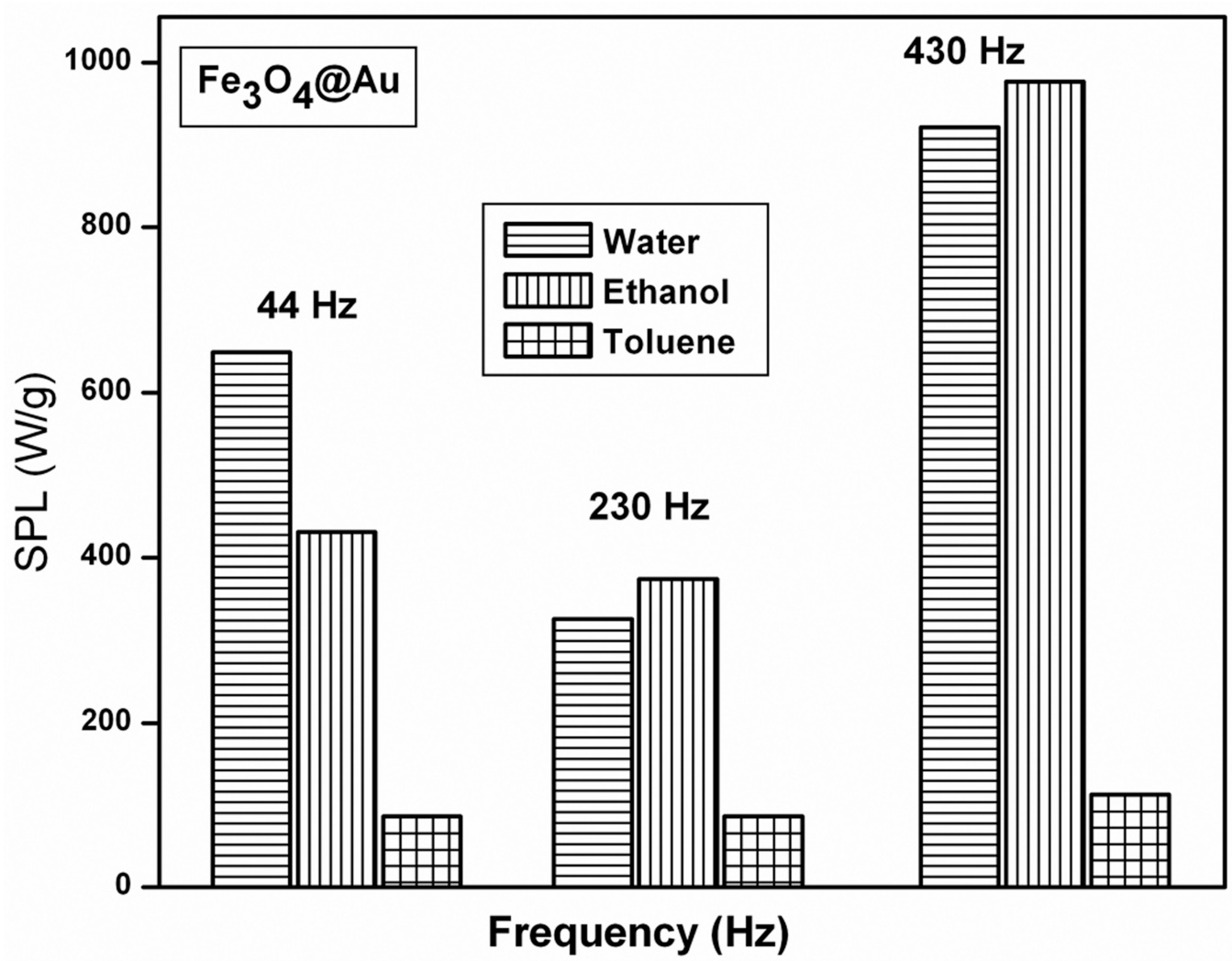

Figure 7.
Solvent dependent SPL values for SPIONs@Au

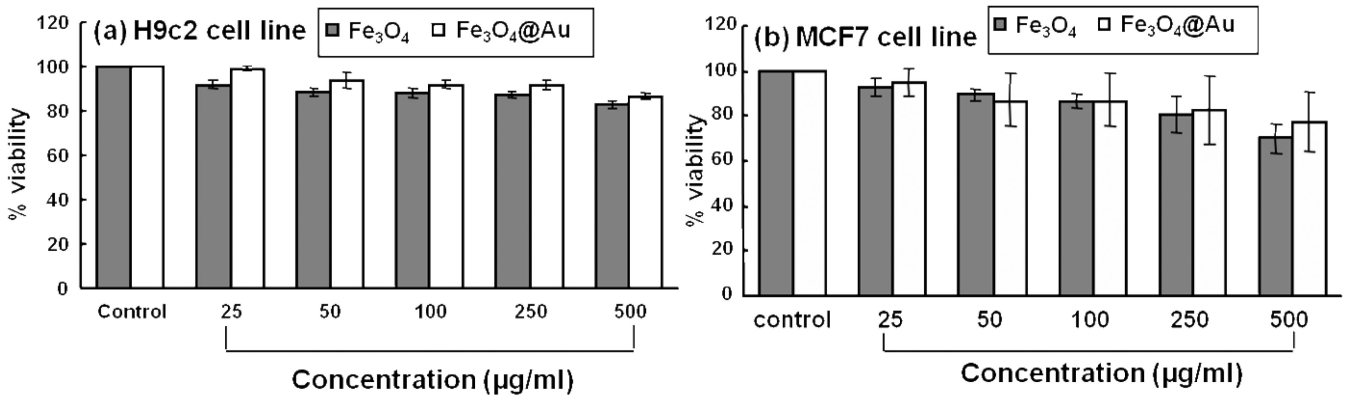

Figure 8.
In vitro toxicity comparison of SPIONs and SPIONs@Au at different concentrations (a) with H9c2 cardiomyoblast cell line and (b) MCF-7 breast carcinoma cells.

Table 1

The average SPL values of SPIONs & SPIONs@Au at different frequencies:

Frequency	Fe_3O_4	Fe_3O_4@Au
44Hz	256.81 W/g	444.32 W/g
230Hz	249.8 W/g	317.75 W/g
430Hz	313.5 W/g	463.9 W/g

Table 2

The average SPL values of SPIONs@Au in different solvent medium at different frequencies:

1.0mg of Fe_3O_4@Au	Water	Ethanol	Toluene
44Hz	648.6 W/g	431 W/g	86.6 W/g
230 Hz	325.5 W/g	374.1 W/g	86.6 W/g
430Hz	920.7 W/g	976 W/g	113 W/g